

Gradual suppression of antiferromagnetism in $\text{BaFe}_2(\text{As}_{1-x}\text{P}_x)_2$: Zero-temperature evidence for a quantum critical point

Tetsuya Iye,^{1,2,*} Yusuke Nakai,^{1,2} Shunsaku Kitagawa,^{1,2} Kenji Ishida,^{1,2} Shigeru Kasahara,³ Takasada Shibauchi,¹ Yuji Matsuda,¹ and Takahito Terashima³

¹*Department of Physics, Graduate School of Science, Kyoto University, Kyoto 606-8502, Japan*

²*TRIP, JST, Sanban-cho Building, 5, Sanban-cho, Chiyoda, Tokyo 102-0075, Japan*

³*Research Center for Low Temperature and Materials Sciences, Kyoto University, Kyoto 606-8502, Japan*

(Received 29 June 2011; revised manuscript received 24 April 2012; published 4 May 2012)

Static and dynamic magnetic properties of lightly P-substituted $\text{BaFe}_2(\text{As}_{1-x}\text{P}_x)_2$ were systematically investigated by ^{31}P NMR. The averaged internal magnetic field at the P site in the zero-temperature limit evaluated from the broadening of NMR spectra in the antiferromagnetic (AFM) phase is gradually suppressed toward $x \sim 0.35$ with increasing x , which provides definitive evidence for the existence of an AFM quantum critical point (QCP) at $x \sim 0.35$. The location of the AFM QCP is consistent with the previous estimation from temperature dependence of spin dynamics in the normal state, and the superconducting transition temperature T_c takes the maximum around the QCP. Our experiments, revealing a signature of a QCP extending up to room temperature, establish $\text{BaFe}_2(\text{As}_{1-x}\text{P}_x)_2$ as one of the most accessible systems for unraveling the nature of quantum criticality and the relationship between AFM quantum criticality and unconventional superconductivity.

DOI: [10.1103/PhysRevB.85.184505](https://doi.org/10.1103/PhysRevB.85.184505)

PACS number(s): 74.40.Kb, 74.25.nj, 74.70.Xa

The relationship between magnetism and superconductivity is one of the central topics in condensed-matter physics, because unconventional superconductors have been discovered near a magnetic phase. Emergent iron-based superconductors are not exceptional.¹⁻⁴ In a parent compound BaFe_2As_2 , tetragonal-to-orthorhombic structural transition and antiferromagnetic (AFM) ordering occur simultaneously (their transition temperatures are denoted as T_S and T_N , respectively). Chemical substitutions of K for Ba,⁵ Co for Fe,⁶ and P for As⁷ suppress T_S and T_N successively, and a superconducting (SC) phase appears at which these transitions almost disappear.

One of the promising theories for unconventional superconductivity is the pairing induced by AFM spin fluctuations.^{8,9} In this scenario, SC transition temperature T_c is highest at a quantum critical point (QCP) of AFM ordering, since the AFM fluctuations are strongest above the QCP where the AFM ordering occurs at $T = 0$ K. In our previous NMR results on $\text{BaFe}_2(\text{As}_{1-x}\text{P}_x)_2$, which is an unconventional superconductor with line nodes in its SC gap structure,¹⁰⁻¹⁵ the temperature dependence of the nuclear spin-lattice relaxation rate $1/T_1$ in the normal state has suggested the existence of a QCP at $x \sim 0.35$ where T_c takes the maximum.¹⁶ Since $\text{BaFe}_2(\text{As}_{1-x}\text{P}_x)_2$ is extremely clean,^{17,18} it is a suitable system to study intrinsic physics of the iron-pnictide superconductors. Observed anomalous T -linear resistivity at $x \sim 0.35$ ¹⁷ and an increase in the quasiparticle effective mass toward $x \sim 0.35$ ¹⁸ are characteristic phenomena of the systems in proximity to a QCP.^{19,20} However, the presence of a QCP requires experimental evidence of second-order quantum phase transition in the zero-temperature limit. A key experiment is to investigate the evolution of an AFM order parameter at the ground state with respect to a physical tuning parameter.

Here, we report ^{31}P -NMR measurements in $\text{BaFe}_2(\text{As}_{1-x}\text{P}_x)_2$ for $0.07 \leq x \leq 0.33$ that bring such direct evidence. Since NMR is a local probe of magnetism at a nuclear site, valuable information on ordered moments can be obtained from an NMR spectrum. The central result

of the present investigation is that an AFM order parameter evaluated above T_c successively decreases upon P substitution toward $x \sim 0.35$, verifying the existence of an AFM QCP by the physical tuning. The present results together with the effective mass enhancement and the temperature dependence of resistivity and $1/T_1$ indicate that $\text{BaFe}_2(\text{As}_{1-x}\text{P}_x)_2$ is an ideal system for unraveling the nature of QCPs and the relationship between quantum criticality and unconventional superconductivity.

We used a collection of single crystals of $\text{BaFe}_2(\text{As}_{1-x}\text{P}_x)_2$ for $x = 0.07, 0.14, 0.20, 0.25, 0.27$, and 0.33 . These are fixed with a GE varnish to prevent sample alignment in the magnetic field. Typical dimension of each single crystal is $100 \times 100 \times 50 \mu\text{m}^3$. ^{31}P -NMR spectra were obtained at a fixed frequency of 71 MHz by sweeping magnetic field around 4.12 T.

To measure SC properties in magnetic fields, the temperature variation of resonance frequency δf of an identical NMR coil, which is proportional to a change in ac-susceptibility, was tracked for $x = 0.14, 0.20, 0.25, 0.27$, and 0.33 at 4.12 T. As shown in Fig. 1(a), SC transitions were detected for $x = 0.20, 0.25, 0.27$, and 0.33 , although the change in δf for $x = 0.20$ does not saturate even at the lowest temperature (1.5 K), suggesting a small volume fraction of SC region in the sample of $x = 0.20$.

Figure 1(b) shows the temperature evolution of ^{31}P -NMR spectra for $x = 0.07-0.27$. The single sharp spectra were observed above each T_N . No remarkable differences between the spectra of $T \geq T_S$ and $T_S \geq T \geq T_N$ were detected within our experimental resolution, where T_S was deduced from a concave kink in the T dependence of resistivity.¹⁷ The Knight shift is almost unchanged against temperature and x in the normal state.²¹ In contrast, each of NMR spectra of $x = 0.07-0.27$ becomes broadened and its intensity decreases below T_N . In the parent BaFe_2As_2 , Fe ordered moments lying in the ab plane with the stripe correlation induce internal magnetic field \mathbf{H}_{int} along the c axis at the As site due to the off-diagonal terms of the hyperfine coupling tensor.²² In

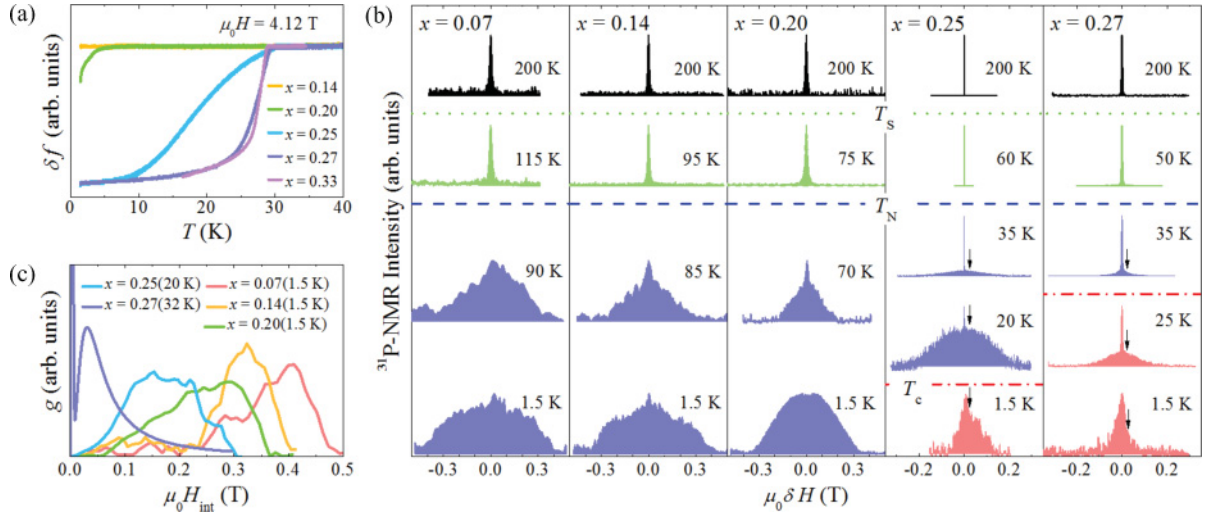


FIG. 1. (Color online) (a) The temperature dependence of Meissner signals for $x = 0.14$ – 0.33 at $\mu_0 H_{\text{int}} = 4.12$ T measured with an identical NMR coil. (b) The temperature dependence of ^{31}P NMR spectra for $x = 0.07$ – 0.27 . The origin of the horizontal axis of each x is set to the temperature-independent peak field of the paramagnetic NMR spectra above T_c . The dotted, broken, and chain lines denote T_S , T_N , and T_c , respectively. The black arrows indicate the resonance field $\mu_0 H \sim 4.14$ T, where T_1 in the magnetically ordered state is measured site-selectively. (c) The distribution of magnetic volume fraction with H_{int} at the P site $g(H_{\text{int}})$ which is deduced from the ^{31}P NMR spectra of $x = 0.07, 0.14$, and 0.20 at 1.5 K, $x = 0.25$ at 20 K, and $x = 0.27$ at 32 K. $\mu_0 H_{\text{int}}$ integral of each $g(H_{\text{int}})$ spectrum is normalized.

such a commensurate AFM ordered state with a homogeneous amplitude of H_{int} at the P site, a powder pattern of $I = 1/2$ becomes nearly rectangular in shape for the case in which H_{int} is negligibly smaller than the applied magnetic field. Such NMR spectra were actually observed in $x = 0.07$ and 0.14 at 1.5 K. However, the rectangular-shaped spectrum turns into a bell-shaped one at $x = 0.20$ and 0.25 , suggestive of a distribution of H_{int} . In the case of an incommensurate AFM order or stripe-type AFM order with distribution of ordered moments, H_{int} at the P site becomes inhomogeneous and the bell-shaped ^{31}P -NMR spectrum is observed, which is composed of a sum of the above commensurate AFM spectra with various internal fields. Therefore, the magnetic volume fraction g with H_{int} can be computed from an observed ^{31}P -NMR spectrum as follows:

$$g(H_{\text{int}}) \propto \left| \delta H \frac{dI(\delta H)}{d\delta H} \right| = \left| H_{\text{int}} \frac{dI(H_{\text{int}})}{dH_{\text{int}}} \right|, \quad (1)$$

where δH is a resonance field measured from the magnetic field of the temperature-independent paramagnetic ^{31}P -NMR spectra above T_N and $I(\delta H)$ is the ^{31}P -NMR intensity at δH . The positive (negative) δH corresponds to H_{int} ($-H_{\text{int}}$). Figure 1(c) shows $g(H_{\text{int}})$ obtained from the NMR spectra of $x = 0.07$ – 0.27 at low temperatures. In $x = 0.25$ and 0.27 , $g(H_{\text{int}})$ is obtained from the NMR spectra above T_c , since the averaged internal field decreases below the bulk T_c as discussed later. Figure 1(c) indicates that the average of internal field decreases, but its distribution seems to increase with increasing x . Such changes might be caused by the change of spin structure from a commensurate to an incommensurate type and/or disorder introduced by P substitution.

Next, we estimate the average of the internal field $\langle H_{\text{int}} \rangle$ from each spectrum in the magnetically ordered state in order to discuss the development of an AFM order parameter. $\langle H_{\text{int}} \rangle$ is calculated as the first moment of each volume fraction

spectrum $g(H_{\text{int}})$:

$$\langle H_{\text{int}} \rangle = \frac{\int_0^\infty H_{\text{int}} g(H_{\text{int}}) dH_{\text{int}}}{\int_0^\infty g(H_{\text{int}}) dH_{\text{int}}} = \frac{\int_0^\infty H_{\text{int}}^2 dI}{\int_0^\infty H_{\text{int}} dI}. \quad (2)$$

The $\langle H_{\text{int}} \rangle$ abruptly increases below T_N and saturates at low temperatures for $x \leq 0.20$, as shown in Fig. 2(a). The temperature dependence of $\mu_0 \langle H_{\text{int}} \rangle$ for $x \leq 0.20$ can be fitted to a conventional behavior of an order parameter $c(T_N - T)^\alpha$. Note that the data of $x = 0.25$ and 0.27 used for the fitting were restricted to range $20 \text{ K} \leq T \leq 50 \text{ K}$ and $31 \text{ K} \leq T \leq 40 \text{ K}$, respectively, since the suppression of $\langle H_{\text{int}} \rangle$ was observed below T_c due to the competition between AFM and SC order parameters (see Ref. 23 for details). The exponent α is shown in the inset of Fig. 2. To investigate the nature of magnetic transition, we measured the temperature dependence of peak intensity of the NMR spectrum for $x = 0.07, 0.14$, and 0.20 on cooling and warming. Sharp decrease in the intensity was observed at T_N for $x = 0.07$ – 0.20 although no appreciable hystereses exceeding an experimental error ($\Delta T \sim 0.5$ K) were observed (not shown here). These results are in contrast to the results of $x = 0$ ²² and indicate that the AFM transitions at T_N in $x = 0.07$ – 0.20 are almost the second-order transitions, consistent with the enhancement of α by the P substitution. $\mu_0 \langle H_{\text{int}} \rangle$ at the ground state, deduced from extrapolating each fitting curve of $\mu_0 \langle H_{\text{int}} \rangle$ to $T \rightarrow 0$ K, is plotted against x in Fig. 3(b). $\mu_0 \langle H_{\text{int}} \rangle$ at $T \rightarrow 0$ K successively decreases from $x = 0.07$ to $x = 0.27$. In contrast to the pronounced increase in $\mu_0 \langle H_{\text{int}} \rangle$ below T_N for $x = 0.07$ – 0.27 , only a slight increase due to SC diamagnetism in $x = 0.33$ indicates the absence of magnetic ordering.

The dynamics of magnetic properties can be probed by measuring the nuclear spin-lattice relaxation rate T_1^{-1} . The time dependence of spin-echo intensity $M(t)$ at the peak of the NMR spectrum after saturation of nuclear magnetization can be fitted to a theoretical curve of nuclear spin $I = 1/2$ with a single component of T_1 . However, for $x = 0.25$ and 0.27 , $M(t)$

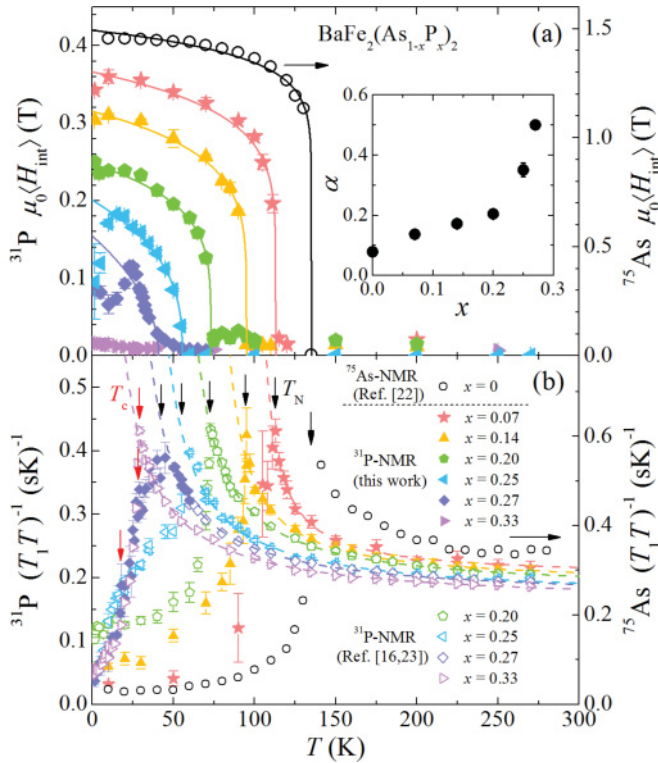


FIG. 2. (Color online) (a) The temperature dependence of the averaged internal magnetic field $\mu_0 \langle H_{\text{int}} \rangle$ at the P site. Internal magnetic field at the As site for $x = 0$ is plotted for comparison (Ref. 22). The solid line for each x is the fitting of the data below T_N to the phenomenological expression $c(T_N - T)^\alpha$. The inset shows x dependence of α . (b) The temperature dependence of ^{31}P $(T_1 T)^{-1}$ in $x = 0.07$ – 0.27 along with ^{75}As $(T_1 T)^{-1}$ in $x = 0$ (Ref. 22) and our previous works on ^{31}P $(T_1 T)^{-1}$ in $x = 0.20, 0.25, 0.27$, and 0.33 are also plotted (Refs. 16 and 23). The broken line for each x is the fitting of the plots to the expected equation for two-dimensional AFM spin fluctuation $(T_1 T)^{-1} = a + b/(T + \theta)$ (Ref. 8). For $x = 0.27$, the data above 65 K were used for the fitting. The black and red arrows indicate T_N and T_c , respectively.

at $T \lesssim 65$ K deviates from the theoretical curves with a single T_1 component due to the inhomogeneity of samples originating from distribution of P concentration. Since the x dependence of T_N is quite steep at around $x \sim 0.26$, a slight distribution of P concentration may cause the phase separation around T_N , resulting in T_1 distribution at low T . Thus, T_1 for $x = 0.25$ and 0.27 in this report was measured site-selectively at the AFM region, which is 0.02 T higher than the sharp peak since the AFM region is dominant at low temperatures. The obtained relaxation curves in the AFM region were nicely fitted with a single T_1 component down to the lowest temperature.

The temperature dependence of $(T_1 T)^{-1}$ is shown for each x in Fig. 2(b). $(T_1 T)^{-1}$ is expressed by the wave-vector \mathbf{q} integral of the imaginary part of the dynamical susceptibility $\chi''(\mathbf{q}, \omega)$. Thus, the Curie-Weiss behavior of $(T_1 T)^{-1}$ and the temperature-independent Knight shifts related to $\chi(\mathbf{q} = 0)$ in the normal state indicate the development of low-energy AFM fluctuations.²¹ On further cooling, the samples for $x = 0.07$ – 0.27 exhibit magnetic ordering, which is inferred from the peaks of $(T_1 T)^{-1}$ at T_N due to slowing down of the

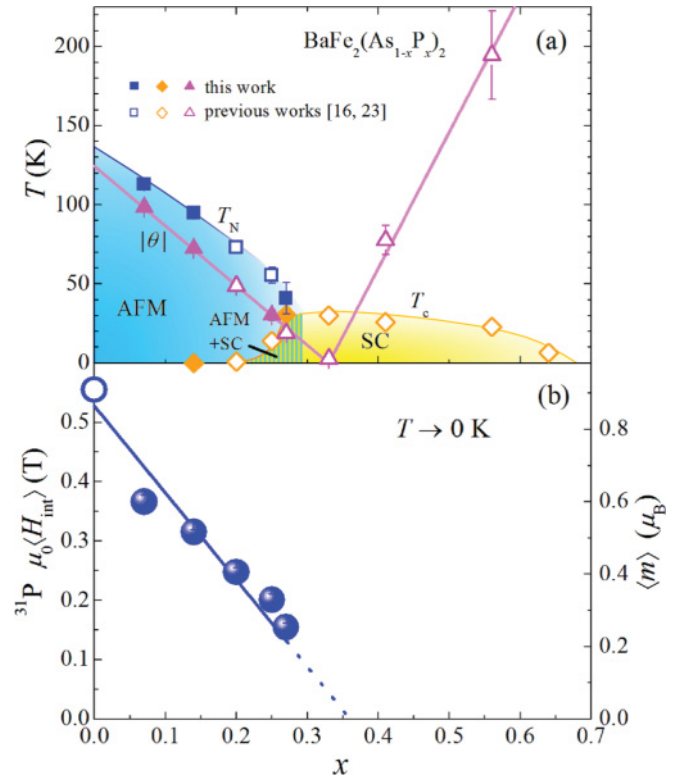


FIG. 3. (Color online) (a) T - x phase diagram of $\text{BaFe}_2(\text{As}_{1-x}\text{P}_x)_2$ determined from our NMR measurements. The filled (open) triangles represent the characteristic temperature of AFM fluctuations $|\theta|$ inferred from $(T_1 T)^{-1}$ in this (previous) work (see text) (Refs. 16 and 23). (b) The x dependence of $\mu_0 \langle H_{\text{int}} \rangle$ at $T \rightarrow 0$ K obtained by extrapolating the fitting curve in Fig. 2(a). The right axis represents the value of the ordered moment $\langle m \rangle = \mu_0 \langle H_{\text{int}} \rangle / {}^3A_{\text{hf}}$, where ${}^3A_{\text{hf}} = 0.61 T/\mu_B$ is deduced using $\langle m \rangle = 0.60 \mu_B$ for $x = 0.08$ (Ref. 24). The magnetic moment of $x = 0, 0.91 \mu_B$, is taken from Ref. 25. The gradual decrease in $\mu_0 \langle H_{\text{int}} \rangle$ at $T \rightarrow 0$ K from $x = 0$ to 0.27 can be extrapolated to $x \sim 0.35$. The broken line is a guide for the eyes.

stripe-type AFM spin fluctuations, whereas $(T_1 T)^{-1}$ in the $x = 0.27$ sample drops sharply at T_c due to the opening of the SC gap. The Curie-Weiss behavior of $(T_1 T)^{-1}$ is well fitted up to room temperature by the equation anticipated for two-dimensional AFM spin fluctuations, $(T_1 T)^{-1} = a + b/(T + \theta)$, where θ denotes the characteristic temperature of AFM fluctuations.⁸

In Fig. 3, we summarize our NMR data of the x dependence of $|\theta|$, $\mu_0 \langle H_{\text{int}} \rangle$ at $T \rightarrow 0$ K, and the ordered moments $\langle m \rangle$ together with the T - x phase diagram of $\text{BaFe}_2(\text{As}_{1-x}\text{P}_x)_2$. It should be noted that $\mu_0 \langle H_{\text{int}} \rangle$ at $T \rightarrow 0$ K is directly related to the AFM order parameter $\langle m \rangle$. We estimated $\langle m \rangle$ using the relation $\mu_0 \langle H_{\text{int}} \rangle = {}^3A_{\text{hf}} \langle m \rangle$, where ${}^3A_{\text{hf}}$ is the off-diagonal term of the hyperfine coupling tensor at the P site and is assumed to be independent of x . ${}^3A_{\text{hf}}$ is calculated to be $0.61 T/\mu_B$ from the ordered moment of $x = 0.08$ ($0.60 \mu_B$) reported from the elastic neutron scattering measurements.²⁴ As shown in Fig. 3(b), $\langle m \rangle$ at $T \rightarrow 0$ K is systematically suppressed toward $x \sim 0.35$, suggestive of the existence of an AFM QCP at $x \sim 0.35$. This is also consistent with a linear suppression of $|\theta|$ down to 0 K at $x \sim 0.35$. Our NMR results clearly demonstrate that the AFM QCP is present at $x \sim 0.35$ and that P substitution

for As acts as a tuning parameter for quantum phase transition in BaFe_2As_2 . As pointed out previously,¹⁶ it is noteworthy that the maximum T_c is observed near the QCP, suggestive of the AFM quantum critical fluctuations playing a vital role for the occurrence of superconductivity in $\text{BaFe}_2(\text{As}_{1-x}\text{P}_x)_2$. The importance of AFM critical fluctuations for superconductivity appears to be a common feature of the “122” iron-pnictide superconductors, since a maximum T_c at around a doping level where T_N disappears was also reported in $\text{Ba}(\text{Fe}_{1-x}\text{T}_x)_2\text{As}_2$ ($T =$ transition metal).^{26,27}

We comment that the interplay between magnetism and superconductivity seems to be quite different between the “122” and “1111” superconductors. The importance of AFM fluctuations to superconductivity in “122” discussed above should be compared with a weak correlation between AFM spin fluctuation and superconductivity in “1111”.²⁸ The phase diagrams of the “1111” iron-pnictide superconductors are essentially different from those of the “122” superconductors; T_S and T_N abruptly disappear as if structural and magnetic transitions are the first-order transition and superconductivity appears suddenly in $\text{LaFeAsO}_{1-x}\text{F}_x$.^{29,30} Furthermore, superconductivity in $\text{CeFeAs}(\text{O}_{1-x}\text{F}_x)$ seems to appear after disappearance of magnetic ordering.³¹

Finally, we point out that in $\text{BaFe}_2(\text{As}_{1-x}\text{P}_x)_2$, the quantum critical fluctuation extends up to room temperature in $x = 0.33$ as can be confirmed by the excellent fitting of the T_1 data up to 270 K with the theoretical curve of 2D AFM fluctuation and T -linear resistivity.¹¹ This is contrary to naive expectations

for quantum phase transition realized at 0 K. Such robust quantum criticality up to high temperatures of the order of J/k_B , where J is the strength of the exchange interaction, is in fact suggested by theoretical study.³² Since the exchange interaction of iron pnictides was estimated to be the order of 100 K,³³ our finding of robust quantum criticality in $\text{BaFe}_2(\text{As}_{1-x}\text{P}_x)_2$ is not unexpected. The present material thus provides an accessible route to unraveling the nature of quantum criticality and emergent quantum order such as unconventional superconductivity.

In summary, static and dynamic magnetic properties in lightly P-substituted $\text{BaFe}_2(\text{As}_{1-x}\text{P}_x)_2$ ($0.07 \leq x \leq 0.33$) were investigated by ³¹P NMR. The averaged internal magnetic field at the P site and the characteristic temperature of AFM fluctuations $|\theta|$ decrease successively toward $x \sim 0.35$ with increasing P concentration. These results verify the existence of an AFM QCP at $x \sim 0.35$, suggesting AFM quantum critical spin fluctuations as the pairing glue of Cooper pairs.

We thank K. Kitagawa, H. Ikeda, and Y. Maeno for experimental support and valuable discussions. This work was supported by the Grant-in-Aid for Scientific Research on Innovative Areas “Heavy Electrons” (No. 20102006) from MEXT, for the GCOE Program “The Next Generation of Physics, Spun from Universality and Emergence” from MEXT, and for Scientific Research from JSPS. Y.N. is supported by KAKENHI (No. 23654120).

*tiye@scphys.kyoto-u.ac.jp

¹Y. Kamihara, T. Watanabe, M. Hirano, and H. Hosono, *J. Am. Chem. Soc.* **130**, 3296 (2008).

²J. Paglione and R. L. Greene, *Nature Phys.* **6**, 645 (2010).

³K. Ishida, Y. Nakai, and H. Hosono, *J. Phys. Soc. Jpn.* **78**, 062001 (2009).

⁴D. C. Johnston, *Adv. Phys.* **59**, 803 (2010).

⁵M. Rotter, M. Tegel, and D. Johrendt, *Phys. Rev. Lett.* **101**, 107006 (2008).

⁶A. S. Sefat, R. Jin, M. A. McGuire, B. C. Sales, D. J. Singh, and D. Mandrus, *Phys. Rev. Lett.* **101**, 117004 (2008).

⁷S. Jiang, H. Xing, G. Xuan, C. Wang, Z. Ren, C. Feng, J. Dai, Z. Xu, and G. Cao, *J. Phys.: Condens. Matter* **21**, 382203 (2009).

⁸T. Moriya, Y. Takahashi, and K. Ueda, *J. Phys. Soc. Jpn.* **59**, 2905 (1990).

⁹P. Monthoux, A. V. Balatsky, and D. Pines, *Phys. Rev. Lett.* **67**, 3448 (1991).

¹⁰K. Hashimoto, M. Yamashita, S. Kasahara, Y. Senshu, N. Nakata, S. Tonegawa, K. Ikada, A. Serafin, A. Carrington, T. Terashima, H. Ikeda, T. Shibauchi, and Y. Matsuda, *Phys. Rev. B* **81**, 220501(R) (2010).

¹¹Y. Nakai, T. Iye, S. Kitagawa, K. Ishida, S. Kasahara, T. Shibauchi, Y. Matsuda, and T. Terashima, *Phys. Rev. B* **81**, 020503(R) (2010).

¹²M. Yamashita, Y. Senshu, T. Shibauchi, S. Kasahara, K. Hashimoto, D. Watanabe, H. Ikeda, T. Terashima, I. Vekhter, A. B. Vorontsov, and Y. Matsuda, *Phys. Rev. B* **84**, 060507(R) (2011).

¹³J. S. Kim, P. J. Hirschfeld, G. R. Stewart, S. Kasahara, T. Shibauchi, T. Terashima, and Y. Matsuda, *Phys. Rev. B* **81**, 214507 (2010).

¹⁴Y. Wang, J. S. Kim, G. R. Stewart, P. J. Hirschfeld, S. Graser, S. Kasahara, T. Terashima, Y. Matsuda, T. Shibauchi, and I. Vekhter, *Phys. Rev. B* **84**, 184524 (2011).

¹⁵Y. Zhang, Z. R. Ye, Q. Q. Ge, F. Chen, J. Jiang, M. Xu, B. P. Xie, and D. L. Feng, *Nat. Phys.* **8**, 371 (2012).

¹⁶Y. Nakai, T. Iye, S. Kitagawa, K. Ishida, H. Ikeda, S. Kasahara, H. Shishido, T. Shibauchi, Y. Matsuda, and T. Terashima, *Phys. Rev. Lett.* **105**, 107003 (2010).

¹⁷S. Kasahara, T. Shibauchi, K. Hashimoto, K. Ikada, S. Tonegawa, R. Okazaki, H. Shishido, H. Ikeda, H. Takeya, K. Hirata, T. Terashima, and Y. Matsuda, *Phys. Rev. B* **81**, 184519 (2010).

¹⁸H. Shishido, A. F. Bangura, A. I. Coldea, S. Tonegawa, K. Hashimoto, S. Kasahara, P. M. C. Rourke, H. Ikeda, T. Terashima, R. Settai, Y. Ōnuki, D. Vignolles, C. Proust, B. Vignolle, A. McCollam, Y. Matsuda, T. Shibauchi, and A. Carrington, *Phys. Rev. Lett.* **104**, 057008 (2010).

¹⁹H. Shishido, R. Settai, H. Harima, and Y. Ōnuki, *J. Phys. Soc. Jpn.* **74**, 1103 (2005).

²⁰S. Sachdev and B. Keimer, *Phys. Today* **64**(2), 29 (2011).

²¹T. Iye, Y. Nakai, S. Kitagawa, K. Ishida, H. Ikeda, S. Kasahara, T. Shibauchi, Y. Matsuda, and T. Terashima (unpublished).

²²K. Kitagawa, N. Katayama, K. Ohgushi, M. Yoshida, and M. Takigawa, *J. Phys. Soc. Jpn.* **77**, 114709 (2008).

²³T. Iye, Y. Nakai, S. Kitagawa, K. Ishida, S. Kasahara, T. Shibauchi, Y. Matsuda, and T. Terashima, *J. Phys. Soc. Jpn.* **81**, 033701 (2012).

²⁴S. Ibuka, T. J. Sato *et al.*, (private communication).

²⁵K. Matan, R. Morinaga, K. Iida, and T. J. Sato, *Phys. Rev. B* **79**, 054526 (2009).

- ²⁶P. C. Canfield and S. L. Bud'ko, *Annu. Rev. Condens. Matter Phys.* **1**, 27 (2010).
- ²⁷F. L. Ning, K. Ahilan, T. Imai, A. S. Sefat, M. A. McGuire, B. C. Sales, D. Mandrus, P. Cheng, B. Shen, and H.-H. Wen, *Phys. Rev. Lett.* **104**, 037001 (2010).
- ²⁸Y. Nakai, K. Ishida, Y. Kamihara, M. Hirano, and H. Hosono, *J. Phys. Soc. Jpn.* **77**, 073701 (2008).
- ²⁹H. Luetkens, H.-H. Klauss, M. Kraken, F. J. Litterst, T. Dellmann, R. Klingeler, C. Hess, R. Khasanov, A. Amato, C. Baines, M. Kosmala, O. J. Schumann, M. Braden, J. Hamann-Borrero, N. Leps, A. Kondrat, G. Behr, J. Werner, and B. Büchner, *Nature Mater.* **8**, 305 (2009).
- ³⁰Y. Nakai, S. Kitagawa, T. Iye, K. Ishida, Y. Kamihara, M. Hirano, and H. Hosono, *Phys. Rev. B* **85**, 134408 (2012).
- ³¹J. Zhao, Q. Huang, C. de la Cruz, S. Li, J. W. Lynn, Y. Chen, M. A. Green, G. F. Chen, G. Li, Z. Li, J. L. Luo, N. L. Wang, and P. Dai, *Nature Mater.* **7**, 953 (2008).
- ³²A. Kopp and S. Chakravarty, *Nature Phys.* **1**, 53 (2005).
- ³³M. D. Lumsden and A. D. Christianson, *J. Phys.: Condens. Matter* **22**, 203203 (2010).